Hydrogen-Bonding Effects on Infrared Spectra from Anharmonic Computations: Uracil–Water Complexes and Uracil Dimers

ARTICLE *in* THE JOURNAL OF PHYSICAL CHEMISTRY A · APRIL 2015

Impact Factor: 2.69 · DOI: 10.1021/acs.jpca.5b01561 · Source: PubMed

4 AUTHORS:

Teresa Fornaro
Carnegie Institution for Science
10 PUBLICATIONS **33** CITATIONS
SEE PROFILE

Diletta Burini
Politecnico di Torino
9 PUBLICATIONS **5** CITATIONS
SEE PROFILE

Malgorzata Biczysko
Shanghai University
84 PUBLICATIONS **1,724** CITATIONS
SEE PROFILE

Vincenzo Barone
Scuola Normale Superiore di Pisa
773 PUBLICATIONS **44,695** CITATIONS
SEE PROFILE

THE JOURNAL OF PHYSICAL CHEMISTRY A

Article

pubs.acs.org/JPCA

Hydrogen-Bonding Effects on Infrared Spectra from Anharmonic Computations: Uracil−Water Complexes and Uracil Dimers

Published as part of The Journal of Physical Chemistry A virtual special issue "Spectroscopy and Dynamics of Medium-Sized Molecules and Clusters: Theory, Experiment, and Applications".

Teresa Fornaro,[†] Diletta Burini,[‡] Malgorzata Biczysko,*[,§,∥] and Vincenzo Barone*[,†]

[†]Scuola Normale Superiore, Piazza dei Cavalieri 7, I-56126 Pisa, Italy

[‡]Dipartimento di Matematica e Informatica, Università di Perugia, INFN Sezione Perugia Via Vanvitelli, I-106123 Perugia, Italy

[§]Physics Department, and International Centre for Quantum and Molecular Structures, Shanghai University, 99 Shangda Road, Shanghai, 200444 China

[∥]Consiglio Nazionale delle Ricerche, Istituto di Chimica dei Composti OrganoMetallici (ICCOM-CNR), UOS di Pisa, Area della Ricerca CNR, Via G. Moruzzi 1, I-56124 Pisa, Italy

Supporting Information

ABSTRACT: Hydrogen-bonding interactions lead to significant changes in the infrared (IR) spectrum, like frequency shifts of the order of magnitude of hundreds of cm^{-1} and increases of IR intensity for bands related to vibrational modes of functional groups directly involved in the hydrogen-bonded bridges. We are actively developing a comprehensive and robust computational protocol aimed at the quantitative reproduction of the spectra of bio-organic and hybrid organic/inorganic molecular systems with a proper account of the variety of intra- and intermolecular interactions. We have resorted to fully anharmonic quantum mechanical computations within the generalized second-order vibrational perturbation theory (GVPT2) approach, combined with the B3LYP-D3 method, in conjunction with basis sets of double-ζ plus polarization quality. Such an approach has been validated in a previous work (*Phys. Chem. Chem. Phys.* **2014**, *16*, 10112−10128) for simulating the IR spectra of the monomers of nucleobases and some of their dimers. In the present contribution we have extended our computational protocol toward hybrid models, with the harmonic part computed at the B2PLYP level, in conjunction with the maug-cc-pVTZ basis set, or by a cost-effective ONIOM B2PLYP:B3LYP focused model, where only part of the molecular system forming the hydrogen bonds is treated at the B2PLYP level of theory. In this work experimental frequencies available for a set of four uracil−water complexes have been considered as references for the computational methodologies applied to the simulation of hydrogen-bonding effects on the infrared spectrum, obtaining average uncertainties of about 22 cm^{-1} for B3LYP-D3/N07D and improved description within 10 cm^{-1} by hybrid B2PLYP/B3LYP-D3 approaches. The same computational schemes have been next applied to simulate fully anharmonic IR spectra of six different hydrogen-bonded uracil dimers, providing reliable support for future experimental investigations on hydrogen-bonded systems.

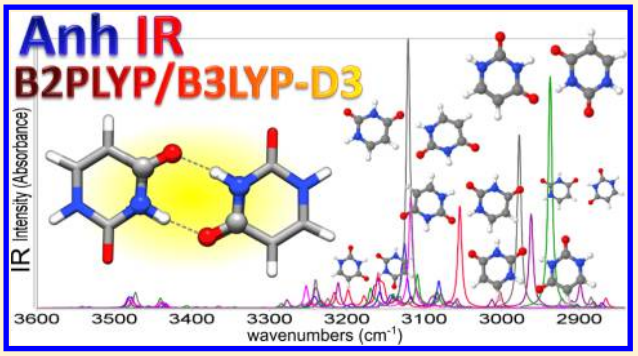

1. INTRODUCTION

Computational spectroscopy techniques play an increasing role in the study of the physical and chemical properties of complex systems dominated by different kinds of intermolecular interactions, because they allow us to dissect the various contributions to the spectroscopic signals, shedding light on the intricate experimental data.[1−12] Among the weak intermolecular interactions, hydrogen bonding acts as important factor in several fields, ranging from materials science, nanotechnology, and surface science to biotechnology, drug design and delivery, and prebiotic chemistry.[13−23] Especially in biological systems, the formation of strong hydrogen bonds can be a crucial driving force for many fundamental processes like protein folding and misfolding or the biological information transfer mechanisms by nucleic acids.[24−27] In the prebiotic context, hydrogen-bonding interactions play a fundamental role in the processes of self-organization and self-interaction of biomolecules, which in turn are responsible for the evolution from the inanimate matter to the biological systems.[28] In particular, nucleobases are very interesting chemical systems that can interact through hydrogen bonds, capable of self-assembling forming dimers, monolayers,or more complex three-dimensional structures.[29,30]

Received: February 15, 2015
Revised: April 12, 2015
Published: April 13, 2015

DOI: 10.1021/acs.jpca.5b01561
J. Phys. Chem. A 2015, 119, 4224−4236

Recently, nucleobases have attracted increasing interest also for the development of biosensors,[31−34] and as biomaterials forming nanostructures for homogeneous dense surface coatings, bottom-up nanopatterning, and 3D nanoparticle lattices.[35]

The hydrogen-bonded complexes of nucleobases with water or their dimers represent the simplest systems for studying the effect of hydrogen-bonding interactions on physicochemical properties like the vibrational features (see, for example, refs 26 and 36−43 and references therein). From the computational point of view, these systems are small enough to allow the use of accurate quantum mechanical (QM) methods for investigating vibrational properties beyond the harmonic approximation, within the second-order vibrational perturbative (VPT2)[44,45] or vibrational self-consistent field (VSCF) based[46−49] approaches. In particular, our group has developed a general VPT2 framework to compute thermodynamic properties, vibrational energies, and transition intensities from the vibrational ground state to fundamentals, overtones and combination bands,[50,51] allowing also for effective computations of large molecular systems within reduced-dimensionality schemes.[52] The information about the intensities of overtones and combination transitions, not available from computations based on the double-harmonic approximation, is required to reproduce the overall band pattern and might be necessary to correctly analyze experimental outcomes, distinguishing low-intensity features related to nonfundamental transitions of the most populated species present in experimental mixtures from fundamental transitions of the less abundant ones.[12,53−57]

It is worth noting that quite remarkable effects of hydrogen-bonding interactions on the infrared (IR) spectrum are usually observed experimentally.[58−60] Indeed, the red shift and intensity enhancement in the X−H stretching frequency following X−H···Y hydrogen bond formation are included among the criteria based on spectroscopy in recent IUPAC definition for hydrogen bond formation.[61] A reliable theoretical description of the relative spectroscopic features is highly desirable to correctly interpret experimental outcomes.[43,62] However, the vibrational treatment of hydrogen-bonded systems is particularly demanding, due to enhanced anharmonicity and accuracy requirements of the underlying potential energy surface (PES).[63]

In a previous work[43] we have studied the IR spectroscopic properties of the isolated nucleobases adenine, hypoxanthine, uracil, thymine, and cytosine, and some of the most stable hydrogen-bonded and stacked dimers of adenine and uracil, identifying a general, reliable, and effective computational procedure based on fully anharmonic QM computations of the vibrational wavenumbers and IR intensities through the generalized second-order vibrational perturbation theory (GVPT2) approach.[12,51] The VPT2 model is particularly appealing for treating medium-size semirigid systems when combined with a semidiagonal fourth-order normal mode representation of the anharmonic force field evaluated by means of density functional theory (DFT) using hybrid functionals in conjunction with polarized double-ζ basis sets (see, for instance, ref 12 and references therein). Fully anharmonic computations employing B3LYP[64] functional in conjunction with N07D[65] or SNSD[12] basis sets have been extensively validated for the prediction of vibrational frequencies with the accuracy necessary for a quantitative comparison with experimental data for systems of increasing size and complexity (see, for instance, refs 12, 66, and 67 and references therein). Several recent results demonstrate that fully anharmonic computations at the VPT2 level provide also realistic IR spectral band shapes[12,68] as well as reliable IR intensities of fundamental transitions, overtones, and combination bands.[69] Moreover, it has been shown that the inclusion of a semiempirical dispersion treatment[70] improves the accuracy of structural parameters and binding energies for systems involving dispersion interactions,[71−73] retaining the same accuracy of the noncorrected methods for the anharmonic frequencies.[12,42,43,72] In particular, the B3LYP-D3/SNSD method has been used to study the hydrogen-bonded and stacked dimers of adenine and uracil, showing energy properties in very good agreement with the best theoretical estimates and providing much better predictions of binding energies and structural parameters than B3LYP/SNSD, not only for stacked structures but also for hydrogen-bonded dimers.[43] The pseudopotential based (DCP) method B3LYP-DCP/6-31+G(2d,2p)[74] has shown very good performance for structural parameters and binding energies of nucleobases dimers as well, but a lower accuracy for vibrational properties. However, B3LYP-DCP/6-31+G(2d,2p) has been shown to outperform several other dispersion-corrected DFT approaches for calculating anharmonic vibrational frequencies, and to provide reliable anharmonic corrections.[43] Therefore, in addition to B3LYP-D3/N07D, we have considered also B3LYP-DCP/6-31+G(2d,2p) (using the new parameters developed by DiLabio and co-workers[75]) for calculating anharmonic vibrational properties. Moreover, improved description of the overall anharmonic frequencies has been achieved through a hybrid scheme[12,76,77] in which the harmonic part of the force-field is computed at a higher level of theory, namely with the double-hybrid B2PLYP functional[78,79] in conjunction with the maug-cc-pVTZ basis set.[80] Within hybrid approaches we have considered also improved description of harmonic frequencies for modes involved in hydrogen-bonding interactions through cost-effective ONIOM B2PLYP:B3LYP computations. Experimental frequencies available for a set of four uracil−water complexes have been considered as references for validation of the computational methodologies that provide the best description of the effect of hydrogen-bonding interactions on the IR spectrum. Then, fully anharmonic infrared spectra of six hydrogen-bonded uracil dimers have been simulated, highlighting the influence of different bonding patterns on the overall IR spectra line shapes and the fingerprint features of the specific hydrogen-bonding interactions. In fact, the theoretical infrared spectra simulated in the present work allow us to go beyond simplified analysis of experimental data based on harmonic approximation[40] and support future experimental investigations.

2. COMPUTATIONAL DETAILS

Anharmonic vibrational computations have been performed by a generalization of the well-known VPT2 model[44,45,50,51,81−105] implemented by some of the present authors in the GAUSSIAN suite of programs[50,51,90,91,101,105] and able to compute thermodynamic and kinetic properties, vibrational energies, and transition intensities from the vibrational ground state to fundamentals, overtones, and combination bands. The semidiagonal quartic force fields have been obtained by numerical differentiation of the analytical second derivatives along each active normal coordinate (with the standard 0.01 Å step) at geometries optimized with tight convergence criteria. Fermi resonances have been treated within the generalized

DOI: 10.1021/acs.jpca.5b01561
J. Phys. Chem. A 2015, 119, 4224−4236

VPT2 scheme (GVPT2), where the nearly resonant contributions are removed from the perturbative treatment (leading to the deperturbed model, DVPT2) and variationally treated in a second step.[50,85,90,92] This model[50,90,91] provided accurate vibrational wavenumbers for several semirigid systems.[12,43,66,106−111] Such an approach relies on semiempirical thresholds for first-order resonances. In the present work, the criteria proposed by Martin et al.[92] for Fermi resonances have been chosen as they provide accurate results for fundamental transitions,[12,111] overtones, and combination bands.[57,105,112] Recently, the method has been extended to compute anharmonic IR, vibrational circular dichroism (VCD), and Raman intensities for the fundamentals, overtones, and combination bands.[12,51,101,105] The computation of IR intensities within the DVPT2 model employs thresholds for 1−1 resonances ranging between 2 and 10 cm^{-1}, to get converged results.

In a first step, geometry optimizations followed by harmonic and anharmonic vibrational calculations at various levels of theory were performed for a set of four uracil−water complexes used as benchmark. The calculations have been performed using B3LYP,[64] B3LYP-D3,[70,113] B3LYP-DCP,[74,114−116] and M06-2X[117] hybrid functionals in conjunction with double-ζ plus polarization basis sets. The N07D[65,118−120] basis set has been applied for B3LYP, B3LYP-D3, and M06-2X computations, whereas the 6-31+G(2d,2p) basis set has been applied for B3LYP-DCP, as recommended by DiLabio.[74] Anharmonic computations have been also performed with hybrid models,[12,69,76,77,79,109,121] in which the harmonic part is computed at double-hybrid B2PLYP[78,79] level of theory and the anharmonic corrections are evaluated by less expensive B3LYP-D3 or B3LYP-DCP approaches. In view of previous experience on increased basis-set requirements,[68,69,79,122,123] all the B2PLYP computations have been performed with maug-cc-pVTZ basis set[80] in which d functions on hydrogens have been removed. Moreover, considering that for larger systems (i.e., uracil dimers) harmonic frequency calculations at the B2PLYP level can be already computationally too demanding, we have tested the performance of a two-layer ONIOM[124,125] B2PLYP:B3LYP scheme (abbreviated as B2:B3) in which the model system (high level, B2PLYP) corresponds to the part of molecular system directly involved in the hydrogen-bonding interaction, with the whole complex taken as the real system (lower level, B3LYP). Partitioning within the uracil monomer, leading to the definition of the model system, has been always performed along a formally single bond. In total, four different partitioning schemes (1−2, 2−3, 3−4, and 4−6) have been defined (Figure 1). For each B2:B3 ONIOM model harmonic frequencies of the uracil monomer show good agreement with their B2PLYP counterparts (Supporting Information). Further validations, including comparison with experimental data, have been performed for uracil−water complexes, in which the water molecule has been included in the model system. Detailed description of all computational models has been gathered in Table 1, along with corresponding labels.

Then, geometry optimizations together with harmonic and anharmonic vibrational calculations have been carried out also for six hydrogen-bonded uracil dimers applying B3D3 and B2:B3 levels of theory. The structures and numbering schemes of the uracil−water complexes and uracil dimers considered in this work, optimized at the B3LYP-D3/N07D level of theory, are shown in Figure 2, and the corresponding coordinates are reported in the Supporting Information. The binding energies

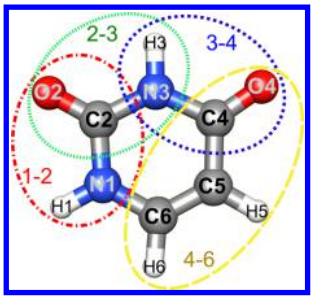

Figure 1. Partitioning schemes of the uracil monomer within ONIOM B2PLYP:B3LYP computations. Parts considered as high level/model systems (computed at the B2PLYP level) are marked by elipses (1−2, 2−3, 3−4, or 4−6).

of uracil dimers have been computed at B3LYP-D3/N07D level of theory as differences between the total energies of the optimized dimer structures and the sums of the total energies of the isolated monomers, taking into account the basis set superposition error (BSSE) via counterpoise correction (CP).[126] Then, such counterpoise-corrected binding energies have been compared to the best theoretical reference values, when available, computed at CCSD(T)/CBS level of theory and reported in the Supporting Information.[127,128]

All calculations have been carried out employing the GAUSSIAN suite of programs.[129] Assignments of vibrational modes were performed by means of visual inspection of the atomic displacements along normal modes and by comparison with the assignments reported in the literature. A graphical user interface (VMS-Draw)[130] has been used to visualize normal modes, analyze in detail the outcome of vibrational computations and draw IR spectra.

3. RESULTS AND DISCUSSION

3.1. Validation of the Computational Method: Uracil−Water Complexes. The set of four uracil−water complexes has been used to benchmark the computational methodologies for simulating the infrared spectroscopic features of hydrogen-bonded systems where strong hydrogen bonds between proton donor and acceptor moieties take place. The availability of the carefully assigned experimental frequencies for isolated uracil−water complexes[41] in the spectral range of NH and OH stretching vibrations allows to assess the performance of different methods in predicting anharmonic vibrational frequencies of functional groups involved in hydrogen-bonding interactions.

The anharmonic vibrational frequencies of the most stable uracil−water complex (complex 1) have been computed at B3, B3D3, B3DCP, M06-2X and hybrid B2/B3D3, B2/B3DCP, and B2:B3 levels of theory (see Table 1 for acronyms). Moreover, harmonic vibrational frequencies have been computed also with the B2PLYP and ONIOM B2:B3 approach. Table 2 reports harmonic and anharmonic OH and NH stretching vibrational frequencies, which are mainly influenced by the hydrogen-bonding interactions, in comparison with their experimental counterparts. The best theoretical description of the effect of hydrogen bonding on the vibrational frequencies has been obtained with the hybrid B2/B3D3 and B2:B3 approaches, providing mean absolute errors (MAEs) with respect to experiment of about 10 cm^{-1}, and maximum discrepancies well below 20 cm^{-1}, further confirming the accuracy of the anharmonic shifts computed with the B3LYP-D3 method. Application of B3LYP-DCP anharmonic correc-

DOI: 10.1021/acs.jpca.5b01561
J. Phys. Chem. A 2015, 119, 4224−4236

Table 1. Description of Computational Models Applied for Computation of Harmonic Frequencies and Anharmonic Corrections

	harmonic		anharmonic	
label	method	basis set	method	basis set
B3	B3LYP	N07D	B3LYP	N07D
B3D3	B3LYP-D3	N07D	B3LYP-D3	N07D
B3DCP	B3LYP-DCP	6-31+G(2d,2p)	B3LYP-DCP	6-31+G(2d,2p)
M062X	M06-2X	N07D	M06-2X	N07D
B2/B3D3	B2PLYP	maug-cc-pVTZ[a]	B3LYP-D3	N07D
B2/B3DCP	B2PLYP	maug-cc-pVTZ[a]	B3LYP-DCP	6-31+G(2d,2p)
B2:B3	ONIOM[b] B2PLYP:B3LYP	maug-cc-pVTZ[a]:N07D	B3LYP-D3	N07D

[a]maug-cc-pVTZ basis set[80] from which the d functions on Hydrogens have been removed. [b]See Figure 1 for partitioning schemes within the ONIOM model.

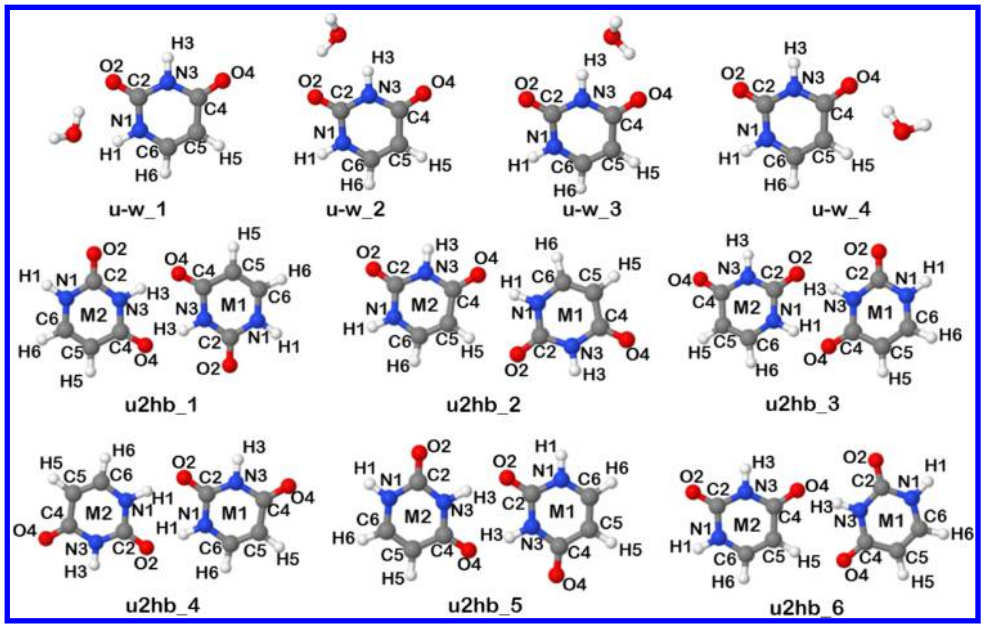

Figure 2. Structures and numbering schemes of the uracil−water and uracil dimers complexes considered in this work, optimized at the B3LYP-D3/N07D level of theory.

Table 2. Harmonic and Anharmonic Vibrational Frequencies in the Spectral Region of NH and OH Stretching Vibrational Modes for the Most Stable Uracil−Water Complex 1, Compared with Experimental Data[a]

		harmonic					
mode[c]	exp[b]	B3	B3D3	B3DCP	M06-2X	B2PLYP	B2:B3
OH	3727	3885	3886	3882	3958	3899	3901
OH (HB)	3468	3600	3604	3591	3710	3626	3629
N3H	3443	3605	3607	3585	3631	3599	3606
N1H (HB)	3317	3428	3423	3405	3480	3451	3454
MAE[d]		141	141	127	206	155	159
|MAX|[e]		162	164	155	243	172	174
		anharmonic					
mode[c]	exp[b]	B3	B3D3	B3DCP	M06-2X	B2/B3D3	B2/B3DCP	B2:B3
OH	3727	3703	3707	3702	3801	3720	3719	3722
OH (HB)	3468	3427	3430	3417	3558	3452	3452	3455
N3H	3443	3439	3440	3419	3497	3432	3433	3439
N1H (HB)	3317	3260	3277	3239	3365	3305	3285	3308
MAE[d]		31	25	44	67	11	16	8
|MAX|[e]		58	40	78	91	16	32	13

[a]See Table 1 for the description of computational models. [b]Experimental data from IR spectra recorded in helium nanodroplets.[41] [c]Modes involved in hydrogen-bonding interactions are labeled as (HB). [d]Mean absolute errors (MAEs) with respect to the experimental data. [e]Maximum absolute deviations (|MAX|) with respect to the experimental data.

DOI: 10.1021/acs.jpca.5b01561
J. Phys. Chem. A 2015, 119, 4224−4236

Table 3. Harmonic and Anharmonic Vibrational Frequencies in the Spectral Region of NH and OH Stretching Vibrational Modes for Uracil−Water Complexes 2−4, Compared with Experimental Data[a]

		harmonic			
mode[c]	exp[b]	B3D3	B3DCP	B2PLYP	B2:B3
Complex 2					
OH	3728	3889	3885	3903	3904
OH (HB)	3501	3647	3635	3667	3671
N1H	3492	3648	3631	3648	3649
N3H (HB)	3256	3420	3393	3430	3439
MAE[d]		157	142	168	172
|MAX|[e]		164	158	175	183
Complex 3					
OH	3722	3887	3883	3900	3902
OH (HB)	3468	3600	3628	3626	3627
N1H	3492	3645	3586	3646	3648
N3H (HB)	3271	3402	3376	3415	3424
MAE[c]		145	130	159	162
|MAX|[d]		164	161	178	180
Complex 4					
OH	3723	3892	3890	3903	3903
OH (HB)	3508	3620	3607	3647	3648
N1H	3492	3644	3628	3644	3645
N3H	3443	3605	3585	3598	3605
MAE[c]		149	136	156	159
|MAX|[d]		169	167	180	180

		anharmonic				
mode[c]	exp[b]	B3D3	B3DCP	B2/B3D3	B2/B3DCP	B2:B3
Complex 2						
OH	3728	3707	3703	3721	3721	3722
OH (HB)	3501	3479	3467	3499	3499	3503
N1H	3492	3480	3464	3480	3481	3481
N3H (HB)	3256	3252	3222	3262	3259	3271
MAE[d]		15	30	7	6	9
|MAX|[e]		22	34	12	11	15
Complex 3						
OH	3722	3705	3701	3718	3718	3720
OH (HB)	3468	3422	3460	3448	3458	3449
N1H	3492	3478	3412	3479	3472	3481
N3H (HB)	3271	3233	3206	3246	3245	3255
MAE[d]		29	43	16	15	12
|MAX|[e]		46	80	25	26	19
Complex 4						
OH	3723	3710	3707	3721	3720	3721
OH (HB)	3508	3459	3444	3486	3484	3487
N1H	3492	3481	3463	3481	3479	3482
N3H	3443	3438	3416	3431	3429	3438
MAE[d]		19	34	12	14	10
|MAX|[e]		49	64	22	24	21

[a]See Table 1 for the description of the computational models. [b]Experimental data from IR spectra recorded in helium nanodroplets.[41] [c]Modes involved in hydrogen-bonding interactions are labeled as (HB). [d]Mean absolute errors (MAEs) with respect to the experimental data. [e]Maximum absolute deviations (|MAX|) with respect to the experimental data.

tions (B2/B3DCP model) leads to slightly worse results, with MAE of 16 cm^{-1} and maximum discrepancy exceeding 30 cm^{-1}.

Among the less expensive methods used in this work, M06-2X yields the worst results, with a MAE of 67 cm^{-1}, whereas the B3LYP-based approaches provide better predictions, with MAEs of 31, 25, and 44 cm^{-1} in the case of B3LYP, B3LYP-D3, and B3LYP-DCP, respectively. In particular, B3LYP-D3 outperforms B3LYP-DCP in calculating the harmonic part of the overall anharmonic frequencies, whereas both methods are roughly equally reliable in the prediction of the anharmonic shifts, as already shown in a previous work.[43]

Thus, we have focused only on B3LYP-D3 and B3LYP-DCP methods for computing anharmonic vibrational frequencies of the other less stable uracil−water complexes (complexes 2−4) reported in Table 3, considering as references for anharmonic computations the hybrid B2/B3D3, B2/B3DCP, and B2:B3 approaches, given their high accuracy compared to the experiment. Similarly to the anharmonic computations for the most stable uracil−water complex, B3D3 provides more

DOI: 10.1021/acs.jpca.5b01561
J. Phys. Chem. A 2015, 119, 4224−4236

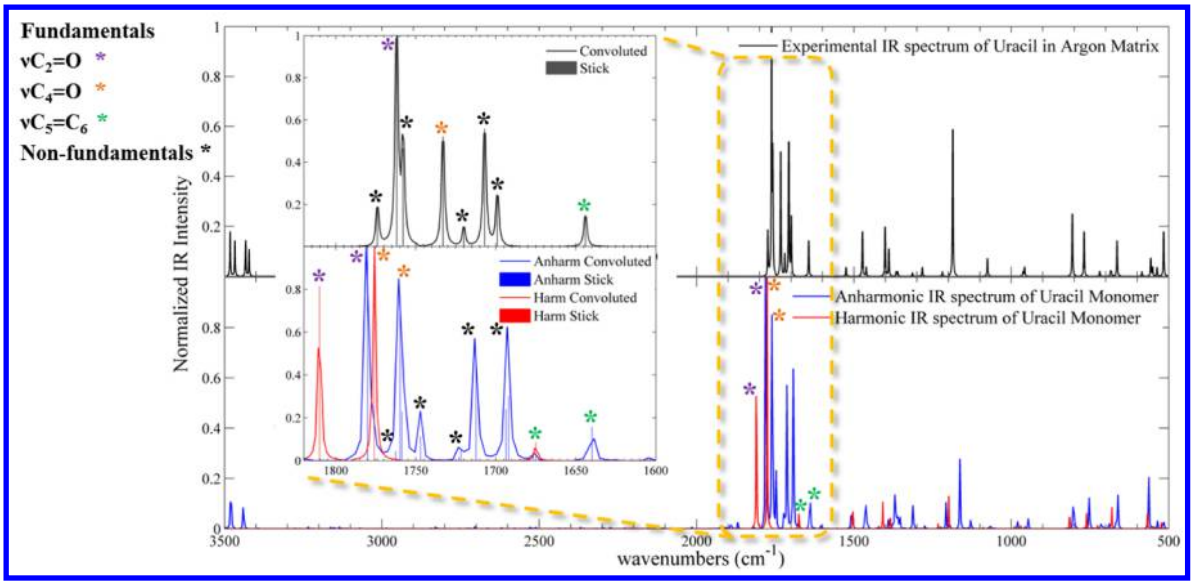

Figure 3. Infrared spectrum of isolated uracil molecule computed with the B3LYP-D3/N07D method, at the harmonic and anharmonic levels, compared with the IR experimental spectrum of uracil isolated in an argon matrix,[133] in the 500−3500 cm^{-1} spectral range, along with the assignment of some IR bands. Experimental IR spectrum recorded in the low-temperature Ar matrix has been generated using the data reported in ref 133. IR spectral line shapes (both theoretical and experimental) have been convoluted using Lorentzian functions with a half-width at a half-maximum (HWHM) of 1 cm^{-1}. The inset shows the 1600−1800 cm^{-1} spectral range, highlighting both stick and convoluted spectra.

accurate results with respect to B3DCP, with MAEs of 15, 29, and 19 cm^{-1} for complexes 2, 3, and 4, respectively, instead of 30, 43, and 34 cm^{-1}, which can be essentially attributed to improvements in the harmonic part. Indeed, the quite similar MAEs obtained using the hybrid B2/B3D3 and B2/B3DCP methods point out the comparable performance of B3LYP-D3 and B3LYP-DCP in predicting the anharmonic corrections. Moreover, it is apparent that the hybrid B2:B3 model, in which the most expensive B2PLYP computations are restricted to the part of molecular system directly involved in hydrogen bond interaction, yields very accurate results, with MAEs of 8−12 cm^{-1} and low maximum absolute deviations with respect to experiments within a range of about 13−21 cm^{-1}. This is due not only to the reliability of the anharmonic shifts computed with the B3LYP-D3/N07D method but also to the increased accuracy of the harmonic part computed through the ONIOM B2:B3 scheme, which is comparable to the accuracy of the full B2PLYP computations, at strongly reduced computational cost.

Results of the anharmonic vibrational computations for the uracil−water complexes indicate that dispersion-corrected B3LYP-based methods are reliable enough for a quantitative comparison with experiments, reproducing well also vibrations involved in hydrogen-bonded bridges that are characterized by more anaharmonic PES with respect to those of the isolated molecules.[59,61,63] In particular, B3LYP-D3 yields more accurate results with average uncertainties within 22 cm^{-1} in the spectral region of hydrogen-bonding interactions. Although B3LYP-DCP/6-31+G(2d,2p) gives higher errors with an average MAE of 38 cm^{-1}, it outperforms several other dispersion-corrected DFT approaches and provides reliable anharmonic corrections. It is worth noting that scaling factors that take into account hydrogen bonding[131] (0.9733 for $\nu(OH)_{free}$ and 0.9602 for ν(OH)-HB do not provide a balanced description of OH stretching vibrations in uracil−water complexes, with mode $\nu(OH)_{free}$ overestimated by up to 65 cm^{-1} and ν(OH)-HB) underestimated by up to 32 cm^{-1}, respectively. The need of a reliable yet not expensive computational method for predicting both the harmonic part and the anharmonic correction to vibrational frequencies suggests B3LYP-D3/N07D as the method of choice.

Then, a more accurate description of the anharmonic frequencies is provided by hybrid computations where the harmonic part of the overall vibrational frequencies is computed at a higher level of theory like B2PLYP. However, to study larger and more complex systems, improved harmonic vibrational frequencies of functional groups involved in the hydrogen-bonding interactions may be obtained by application of the less demanding ONIOM B2:B3 scheme, which is a focused model where only the part of the molecular system forming the hydrogen bonds is treated at the B2PLYP level of theory and the remaining part is treated with B3LYP, obtaining average uncertainties of about 10 cm^{-1} in the spectral region of hydrogen-bonding interactions.

3.2. Effect of Hydrogen-Bonding Interactions on the Infrared Spectrum: Uracil Dimers. Our previous works on nucleobase complexes have already highlighted the remarkable effects of intermolecular interactions, including hydrogen bonds, on the vibrational frequencies of the molecules.[22,28,43,62] In the case of uracil in the solid state,[22,132] such intermolecular interactions are responsible for significant red shifts of the vibrational frequencies with respect to uracil isolated in an argon matrix:[133−135] about 400 cm^{-1} for the NH stretching modes and 80 cm^{-1} for the stretching modes of the carbonyl groups involved in the hydrogen bonds. These experimental shifts have been reproduced quite well theoretically by reduced dimensionality VPT2 approaches using the B3LYP-D3/N07D method, simulating a cluster of seven uracil molecules.[62]

For uracil monomer and the hydrogen-bonded uracil dimers, a full VPT2 anharmonic treatment at B3D3 or B2:B3 levels is feasible, allowing for an improved accuracy of computed vibrational frequencies. In the absence of hydrogen bonds, i.e., in the case of the isolated uracil molecule, the accuracy of fully anharmonic VPT2 calculations using the B3LYP-D3/N07D method is particularly high, about 10 cm^{-1} (all harmonic and

DOI: 10.1021/acs.jpca.5b01561
J. Phys. Chem. A 2015, 119, 4224−4236

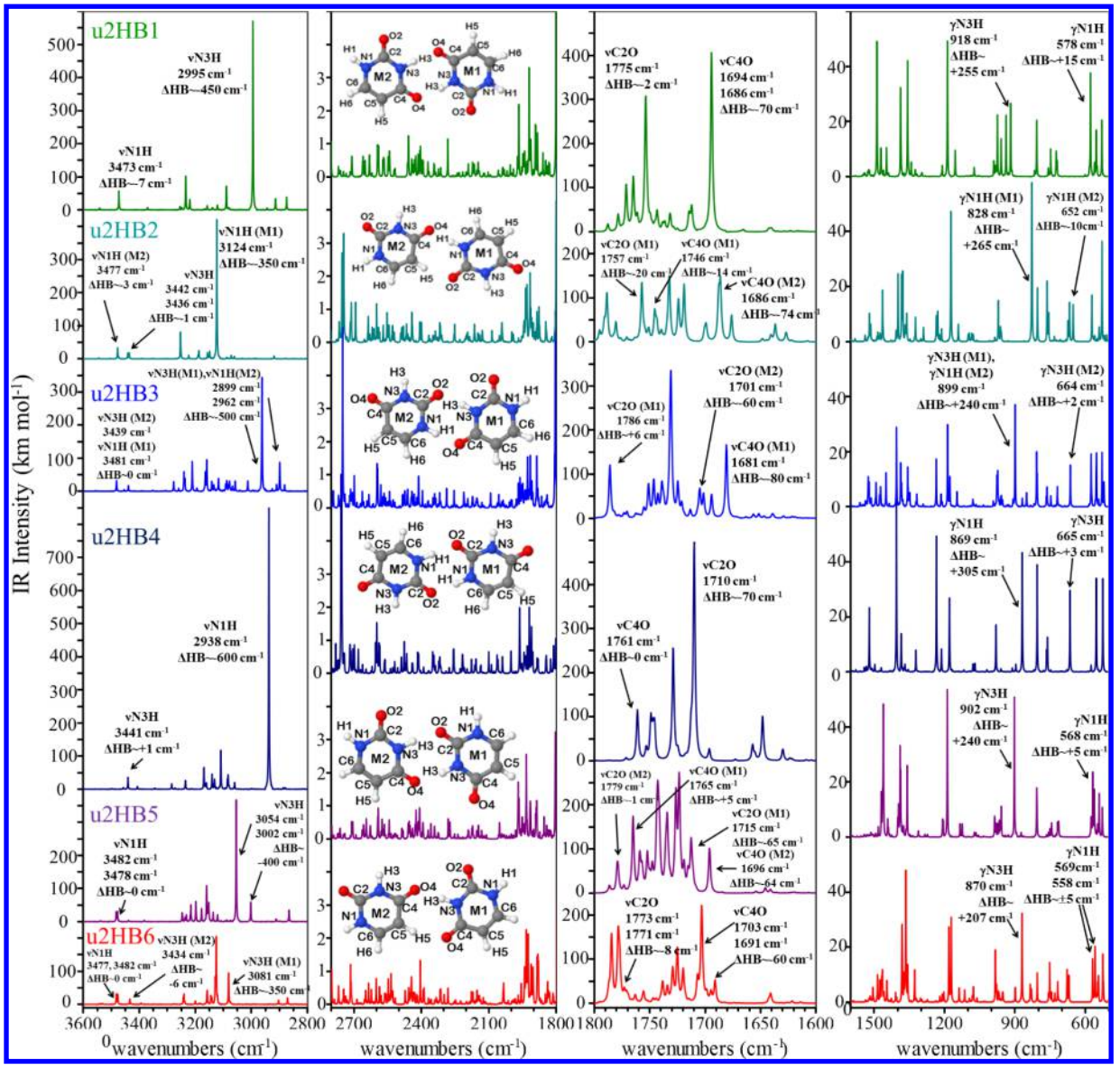

Figure 4. Anharmonic infrared spectra of the six different hydrogen-bonded uracil dimers computed with the B3LYP-D3/N07D method, along with the assignment of the NH and CO stretchings and NH bendings, and the corresponding shifts of the vibrational frequencies with respect to uracil monomer due to the formation of the hydrogen-bonding interactions (ΔHB).

anharmonic vibrational frequencies and IR intensities are reported in the Supporting Information), on par with the much more computationally demanding approaches with the harmonic frequencies evaluated by a composite scheme at the coupled cluster (CC) level (CCSD(T)/CBS(T,Q)+aug +CV).[121] A very good agreement between theory and experiment, is achieved not only for the fundamental transitions but also for the whole IR spectra as shown in Figure 3 comparing the fully anharmonic IR spectrum of the uracil monomer computed at the B3LYP-D3/N07D level of theory with the experimental spectrum of uracil isolated in an argon matrix.[133] In fact, although anharmonic frequencies improve the accuracy of their harmonic counterparts, anharmonic intensities (including both mechanical and electric anharmonic terms) are often needed to obtain even qualitatively correct spectral shapes because overtones and combination bands have vanishing intensities at the harmonic level. The experimental features in the 1600−1800 cm^{-1} spectral range, shown in the inset, are well reproduced by anharmonic calculations, in particular taking into account also the presence of relatively intense non-fundamental transitions. Anharmonic computations show, in addition to the two most intense bands corresponding to the CO stretching fundamentals and one weaker transition related to the ν(C5C6) mode, also five nonfundamental transitions. In line with experimental findings two of them are nearly as intense as the ν(C4O) fundamental. It should be noted that such a result could not be obtained by application of scaling factors to the harmonic frequencies as in this case only the three bands corresponding to the fundamental transitions are present instead of complex pattern including also combination bands and overtones. These results further confirm that GVPT2/DVPT2 anharmonic computations employing DFT potential energy surfaces provide qualitatively correct IR intensities of all transitions, largely sufficient to simulate realistic band patterns. Whenever highly accurate IR intensities are needed, for example, for atmospheric or astrochemical studies, quantitative results can be obtained by hybrid models

DOI: 10.1021/acs.jpca.5b01561
J. Phys. Chem. A 2015, 119, 4224−4236

Table 4. Selected Harmonic and Anharmonic Results Computed for the Hydrogen-Bonded Uracil Dimers[a]

mode[b,c]	B3D3 harm.	B3D3 anh	B3D3 Δanh	B2:B3 harm.	B2:B3 anh	mode[b,c]	B3D3 harm.	B3D3 anh	B3D3 Δanh	B2:B3 harm.	B2:B3 anh
u2hb1						**u2hb4**					
ν(N1H) (M1,M2)	3645	3473	−172	3648	3476	ν(N3H) (M1,M2)	3606	3441	−165	3606	3441
ν(N1H) (M1,M2)	3645	3473	−172	3648	3476	ν(N3H) (M1,M2)	3606	3441	−165	3606	3440
ν(N3H)-HB (M1,M2)	3248	2995	−253	3303	3050	ν(N1H)-HB (M1,M2)	3235	2938	−297	3272	2975
ν(N3H)-HB (M1,M2)	3202	2956	−246	3265	3019	ν(N1H)-HB (M1,M2)	3181	2871	−310	3223	2913
ν(C2O) (M1,M2)	1814	1782	−33	1809	1776	ν(C4O) (M1,M2)	1788	1761	−27	1783	1756
ν(C2O) (M1,M2)	1812	1775	−37	1807	1770	ν(C4O) (M1,M2)	1783	1760	−23	1781	1758
ν(C4O)-HB (M1,M2)	1743	1694	−49	1729	1681	ν(C2O)-HB (M1,M2)	1759	1710	−49	1747	1698
ν(C4O)-HB (M1,M2)	1734	1686	−47	1724	1676	ν(C2O)-HB (M1,M2)	1755	1711	−44	1743	1699
γ(N3H)-HB (M1,M2)	942	918	−24	909	885	γ(N1H)-HB (M1,M2)	907	869	−38	893	854
γ(N3H)-HB (M1,M2)	918	892	−25	885	860	γ(N1H)-HB (M1,M2)	873	832	−40	861	821
γ(N1H) (M1,M2)	582	578	−4	575	571	γ(N3H) (M1,M2)	682	665	−17	677	660
γ(N1H) (M1,M2)	582	578	−4	575	571	γ(N3H) (M1,M2)	682	664	−17	677	660
u2hb2						**u2hb5**					
ν(N1H) (M2)	3641	3477	−164	3643	3479	ν(N1H) (M1)	3647	3482	−165	3648	3483
ν(N1H) (M1)	3610	3441	−168	3610	3441	ν(N1H) (M2)	3645	3478	−168	3648	3481
ν(N3H) (M1)	3604	3436	−168	3604	3436	ν(N3H)-HB (M1,M2)	3288	3054	−233	3337	3104
ν(N3H)-HB (M2)	3292	3123	−169	3326	3157	ν(N3H)-HB (M1,M2)	3242	3002	−240	3302	3062
ν(C2O) (M2)	1817	1780	−36	1814	1778	ν(C2O) (M2)	1813	1779	−34	1807	1773
ν(C2O) (M1)	1787	1757	−30	1760	1730	ν(C2O) (M1)	1782	1765	−17	1776	1759
ν(C4O) (M1)	1767	1746	−21	1776	1754	ν(C4O)-HB (M1)	1768	1715	−52	1755	1702
ν(C4O)-HB (M2)	1727	1686	−41	1709	1668	ν(C4O)-HB (M2)	1740	1696	−44	1728	1685
γ(N1H)-HB (M1)	871	828	−43	863	819	γ(N3H)-HB (M1,M2)	927	902	−25	894	870
γ(N1H)-HB (M1), γ(CH) (M2)	849	826	−23	847	824	γ(N3H)-HB (M1,M2)	901	879	−22	869	848
γ(N3H) (M1)	678	652	−27	673	646	γ(N1H) (M2)	576	568	−9	574	566
γ(N1H) (M2)	590	572	−19	587	568	γ(N1H) (M1)	571	561	−10	566	556
u2hb3						**u2hb6**					
ν(N1H) (M1)	3642	3481	−161	3644	3484	ν(N1H) (M1)	3647	3482	−166	3650	3484
ν(N3H) (M2)	3606	3439	−167	3606	3439	ν(N1H) (M2)	3645	3477	−168	3647	3479
ν(N3H)-HB (M1), ν(N1H)-HB (M2)	3237	2962	−275	3283	3009	ν(N3H) (M2)	3604	3434	−170	3604	3433
ν(N3H)-HB (M1), ν(N1H)-HB (M2)	3186	2899	−287	3240	2953	ν(N3H)-HB (M1)	3289	3081	−208	3332	3125
ν(C2O) (M1)	1820	1786	−34	1814	1780	ν(C2O) (M1,M2)	1812	1773	−39	1809	1770
ν(C2O) (M2)	1782	1755	−27	1777	1750	ν(C2O) (M1,M2)	1810	1771	−39	1805	1766
ν(C4O)-HB (M2)	1764	1701	−62	1754	1691	ν(C4O)-HB (M1,M2)	1755	1703	−51	1737	1685
ν(C4O)-HB (M1)	1728	1681	−48	1717	1669	ν(C4O) (M1,M2)	1738	1691	−47	1721	1674
ν(N3H)-HB (M1), ν(N1H)-HB (M2)	932	899	−33	905	872	γ(N3H)-HB (M1)	910	870	−40	877	837
ν(N1H)-HB (M2), ν(N3H)-HB (M1)	890	850	−40	872	832	γ(N3H) (M2)	687	670	−17	683	666
γ(N3H) (M2)	682	664	−19	677	658	γ(N1H) (M2)	580	569	−11	575	564
γ(N1H) (M1)	591	575	−16	584	569	γ(N1H) (M1)	575	558	−17	569	552

[a]See Table 1 for the description of the computational models. [b]Modes involved in hydrogen-bonding interactions are labeled as (HB). [c]Modes localized on one of the uracil monomers are marked as (M1) and (M2), and modes delocalized over the dimer are labeled as (M1,M2), respectively.

in which the harmonic part is accounted for at the coupled cluster level.[68,69,136]

To investigate the effect of the intermolecular interactions on the vibrational frequencies of nucleobases, the fully anharmonic infrared spectra of six different hydrogen-bonded uracil dimers have been computed at the B3LYP-D3/N07D level of theory and compared to the IR spectrum of the isolated uracil monomer. Figure 4 shows the anharmonic IR spectra of all uracil dimers, along with the assignment of the NH and CO stretching vibrational modes and NH out-of-plane bendings, pointing out the different shifts of the corresponding vibrational frequencies with respect to uracil monomer due to the formation of the hydrogen-bonding interactions (all harmonic and anharmonic vibrational frequencies and IR intensities are reported in the Supporting Information).

An important observation is that, depending on the specific hydrogen bonds, the infrared spectral features are significantly different, and such reliable theoretical simulations can help to distinguish among the different dimers in experimental mixtures.[40] As expected, the most important shifts of the vibrational frequencies and/or IR intensity variations concern the functional groups that are directly involved in the hydrogen-bonding interactions. In particular, the NH modes are extremely sensitive to H-bonding, featuring significant red shifts for the stretching vibrations and analogous blue shifts for the out-of-plane bendings, as already observed in other

DOI: 10.1021/acs.jpca.5b01561
J. Phys. Chem. A 2015, 119, 4224−4236

systems,[137] and used to establish empirical correlations between these spectral parameters and the H-bond properties.[138]

In the case of the u2hb1 dimer, the most significant red shifts with respect to isolated uracil (about 450 and 70 cm^{-1}) are observed in both monomers for modes ν(N3H) at 2995 and 2956 cm^{-1} and ν(C4O) at 1694 and 1686 cm^{-1}, respectively. The N3H and C4O functional groups of the two monomers are, indeed, involved in two strong hydrogen bonds in this dimer. This results in large red shifts for the corresponding vibrational modes, pointing out a weakening of the force constants due to the hydrogen-bonding interactions, and a corresponding increase of IR intensities. On the contrary, the out-of-plane bending modes of the N3H groups (at about 900 cm^{-1}) undergo a corresponding blue shift of about 250 cm^{-1}.

The u2hb2 dimer, instead, features only one hydrogen bond between the N1H group of monomer 1 and the C4O group of monomer 2, and another weaker interaction between the C2O group of monomer 1 and the C5H group of monomer 2. This is clearly spotted in the changes of the spectroscopic features, with the most important red shifts of the vibrational frequencies of about 350 and 74 cm^{-1} concerning the ν(N1H) mode of monomer 1 at 3124 cm^{-1} and ν(C4O) mode of monomer 2 at 1686 cm^{-1}, respectively, which correspond to the most intense IR bands in the spectrum as well. A blue shift of about 260 cm^{-1} has been observed for the γ(N1H) vibration of monomer 1 at about 827 cm^{-1}. Another noteworthy red shift of about 50 cm^{-1} has been observed for the ν(C5H) mode of monomer 2 at 3072 cm^{-1}, along with a less significant 20 cm^{-1} red shift of the ν(C2O) mode of monomer 1 at 1757 cm^{-1}.

The u2hb3 dimer features two hydrogen bonds, one involving the C4O group of monomer 1 and the N1H group of monomer 2 and the other between the N3H group of monomer 1 and the C2O group of monomer 2. This results in two strongly red-shifted, of about 500 cm^{-1}, intermolecular modes at 2962 and 2899 cm^{-1}, corresponding to the combination of modes ν(N3H) of monomer 1 and ν(N1H) of monomer 2, and red shifts of about 80 and 60 cm^{-1} for the ν(C4O) band of monomer 1 at 1681 cm^{-1} and the ν(C2O) mode of monomer 2 at 1701 cm^{-1}, respectively. Also in this case, remarkable blue shifts (above 200 cm^{-1}) have been observed for the γ(NH) vibration involved in the hydrogen-bonds.

The u2hb4 dimer shows the largest red shifts, about 600 cm^{-1}, for the ν(N1H) vibration of both monomers at 2938 and 2871 cm^{-1}, as the result of the formation of two very strong hydrogen-bonds between the N1H and C2O groups of both monomers. Analogously, the ν(C2O) bands of both monomers at 1711 and 1710 cm^{-1} present red shifts of about 70 cm^{-1}. Blue shifts above 250 cm^{-1} have been observed for the γ(N1H) mode of both monomers as well.

The u2hb5 dimer has two hydrogen bonds involving the N3H groups of both monomers and the C2O group of monomer 1 and C4O group of monomer 2, with corresponding red shifts of about 400 cm^{-1} for the modes ν(N3H) at 3054 and 3002 cm^{-1}, 65 cm^{-1} for the mode ν(C2O) of monomer 1 at 1715 cm^{-1}, 64 cm^{-1} for the mode ν(C4O) of monomer 2 at 1696 cm^{-1}, and blue shifts above 200 cm^{-1} for the γ(N3H) vibrations of both monomers.

Finally, the u2hb6 dimer features only one hydrogen bond between the N3H group of monomer 1 and the C4O group of monomer 2, and a weaker intermolecular interaction between the C4O group of monomer 1 and the C5H group of monomer 2, resulting in the most important red shifts of about 350 cm^{-1} for the ν(N3H) mode of monomer 1 at 3081 cm^{-1}, 60 cm^{-1} for both the ν(C4O) modes at 1703 and 1691 cm^{-1}, and a blue shift of about 200 cm^{-1} for the γ(N3H) vibration of monomer 1.

It is worth noting that the magnitude of the vibrational shifts for the modes of functional groups involved in the hydrogen bonds in the dimers can be considered as an indication of the strength of the intermolecular interactions taking place in the complexes, which in turn reflects their relative stability. This is in agreement with the trend of the binding energies of the complexes under study that are reported in the Supporting Information.

All harmonic and anharmonic vibrational frequencies in the region of hydrogen-bonding interactions (NH and CO stretchings and NH bendings) computed with the B3D3 model are also listed in Table 4, along with more accurate results obtained by computing the hybrid anharmonic frequencies at the B2:B3 level of theory, with only a slight increase of the computational burden. The mean absolute deviation of the anharmonic B3D3 frequencies for all the dimers with respect to the hybrid anharmonic frequencies computed at the B2:B3 level of theory is of about 28 cm^{-1} in the specific zone of the hydrogen-bonded functional groups, mainly due to the variation of NH stretching and bending vibrations, by 49 and 22 cm^{-1}, on average, respectively. At variance, for ν(NH), ν(CO), and γ(NH) modes not involved in hydrogen bonding the B3D3 and B2:B3 frequencies agree within 5 cm^{-1}. Thus, the ONIOM B2:B3 scheme can be suggested as an inexpensive method to correct the harmonic part of the vibrational frequencies of functional groups involved in strong hydrogen bonds, using the B3LYP-D3/N07D method for computing the anharmonic corrections to these modes together with all other vibrational frequencies and IR intensities.

4. CONCLUSIONS

The possibility of accurately predicting the effect of hydrogen-bonding interactions on the infrared spectral features is of fundamental importance to interpret experimental data of most systems of interest in biology, drug design, biotechnology, nanosciences, material sciences, and so forth. Usually, hydrogen-bonding interactions cause wide changes in the infrared spectrum, like shifts of the order of magnitude of hundreds of cm^{-1} and significant increases in the intensity of IR bands of vibrational modes of functional groups directly involved in the hydrogen-bonded bridges. An accurate theoretical description of the relative infrared spectroscopic features is highly required to correctly interpret experimental outcomes. The problems of simulating strongly anharmonic vibrations within hydrogen-bonded bridges are related to both possible limitations of the VPT2 treatment and the requirement of a very accurate description of the underlying PES.

This work shows that the GVPT2 model, combined with a semidiagonal fourth-order polynomial representation of the anharmonic force field in terms of normal modes, evaluated by means of density functional theory using the B3LYP-D3 functional in conjunction with the N07D basis set, is reliable enough to describe the vibrational properties of hydrogen-bonded systems like uracil−water complexes, with average uncertainties within 22 cm^{-1} in the spectral region of hydrogen-bonding interactions. An improved description of the harmonic part of the vibrational frequencies of functional groups involved in the hydrogen-bonding interactions has been achieved by

DOI: 10.1021/acs.jpca.5b01561
J. Phys. Chem. A 2015, 119, 4224−4236

application of the ONIOM B2PLYP:B3LYP scheme, which is a focused model where only the part of the molecular system forming the hydrogen bonds is treated at the B2PLYP level of theory. It leads to a definition of inexpensive hybrid approach, with anharmonic corrections computed at B3LYP-D3 level, allowing us to obtain average uncertainties of about 10 cm^{-1} in the spectral region of hydrogen-bonding interactions. Therefore, we have confidently applied these methods to simulate the fully anharmonic infrared spectrum of six different hydrogen-bonded uracil dimers to analyze the differences of their spectra and the changes in the infrared features due to the formation of the hydrogen-bonding interactions. These theoretical predictions and proposed methodology can be useful for supporting future experimental investigations on hydrogen-bonded systems like the uracil dimers.

■ ASSOCIATED CONTENT

Supporting Information

(i) Cartesian coordinates of the equilibrium structures of all complexes optimized at the B3LYP-D3/N07D level. (ii) Counterpoise-corrected binding energies for the optimized structures of the hydrogen-bonded uracil dimers, computed at the B3LYP-D3/N07D level and compared to the best theoretical estimates. (iii) Harmonic and anharmonic vibrational frequencies and IR intensities for the uracil monomer computed with the B3LYP-D3/N07D method, compared with the experimental frequencies, and ONIOM B2:B3 harmonic frequencies compared with B2PLYP ones. (iv) Harmonic and anharmonic vibrational frequencies and IR intensities for the uracil dimers computed with the B3LYP-D3/N07D method. This material is available free of charge via the Internet at http://pubs.acs.org.

■ AUTHOR INFORMATION

Corresponding Authors

*M. Biczysko. E-mail: malgorzata.biczysko@pi.iccom.cnr.it.
*V. Barone. E-mail: vincenzo.barone@sns.it.

Notes

The authors declare no competing financial interest.

■ ACKNOWLEDGMENTS

The research leading to these results has received funding from the European Union's Seventh Framework Programme (FP7/2007-2013) under grant agreement no. ERC-2012-AdG-320951-DREAMS and from Italian MIUR (under the project PON01-01078/8). M.B. acknowledge support of COST CMTS-Action CM1405 (MOLIM: MOLecules In Motion).

■ REFERENCES

(1) Jensen, P.; Bunker, P. R. *Computational Molecular Spectroscopy*; John Wiley and Sons Ltd.: Chichester, U.K., 2000.
(2) Barone, V., Ed. *Computational Strategies for Spectroscopy, from Small Molecules to Nano Systems*; John Wiley & Sons, Inc.: Hoboken, NJ, 2011.
(3) Grunenberg, J., Ed. *Computational Spectroscopy*; Wiley-VCH Verlag GmbH & Co. KGaA: Weinheim, Germany, 2010.
(4) Barone, V.; Baiardi, A.; Biczysko, M.; Bloino, J.; Cappelli, C.; Lipparini, F. Implementation and Validation of a Multi-purpose Virtual Spectrometer for Large Systems in Complex Environments. *Phys. Chem. Chem. Phys.* **2012**, *14*, 12404−12422.
(5) Siebert, F., Hildebrandt, P., Eds. *Vibrational Spectroscopy in Life Science*;Wiley-VCH Verlag GmbH and Co. KGaA: Weinheim, Germany, 2008.
(6) Berova, N., Polavarapu, P. L., Nakanishi, K., Woody, R. W., Eds. *Comprehensive Chiroptical Spectroscopy: Applications in Stereochemical Analysis of Synthetic Compounds:Natural Products, and Biomolecules*; John Wiley & Sons, Inc.: Hoboken, NJ, 2012; Vol. 2.
(7) Laane, J., Ed. *Frontiers of Molecular Spectroscopy*; Elsevier: Amsterdam, 2009.
(8) Watson, M. D.; Fechtenkötter, A.; Müllen, K. Big Is Beautiful "Aromaticity" Revisited from the Viewpoint of Macromolecular and Supramolecular Benzene Chemistry. *Chem. Rev.* **2001**, *101*, 1267−1300.
(9) Elemans, J. A. A. W.; Lei, S.; de Feyter, S. Molecular and Supramolecular Networks on Surfaces: From Two-Dimensional Crystal Engineering to Reactivity. *Angew. Chem., Int. Ed.* **2009**, *48*, 7298−7332.
(10) Iwaura, R.; Iizawa, T.; Minamikawa, H.; Ohnishi-Kameyama, M.; Shimizu, T. Diverse Morphologies of Self-Assemblies from Homoditopic 1,18-Nucleotide-Appended Bolaamphiphiles: Effects of Nucleobases and Complementary Oligonucleotides. *Small* **2010**, *6*, 1131−1139.
(11) Barone, V.; Biczysko, M.; Borkowska-Panek, M.; Bloino, J. A Multifrequency Virtual Spectrometer for Complex Bio-Organic Systems: Vibronic and Environmental Effects on the UV/Vis Spectrum of Chlorophyll-a. *ChemPhysChem* **2014**, *15*, 3355−3364.
(12) Barone, V.; Biczysko, M.; Bloino, J. Fully Anharmonic, IR and Raman Spectra of Medium-size Molecular Systems: Accuracy and Interpretation. *Phys. Chem. Chem. Phys.* **2014**, *16*, 1759−1787.
(13) Donhauser, Z. J.; Mantooth, B. A.; Kelly, K. F.; Bumm, L. A.; Monnell, J. D.; Stapleton, J. J.; Price, D. W.; Rawlett, A. M.; Allara, D. L.; Tour, J. M.; Weiss, P. S. Conductance Switching in Single Molecules Through Conformational Changes. *Science* **2001**, *292*, 2303−2307.
(14) Lehn, J.-M. Toward Complex Matter: Supramolecular Chemistry and Self-organization. *Proc. Natl. Acad. Sci. U. S. A.* **2002**, *99*, 4763−4768.
(15) Kitano, H. Systems Biology: A Brief Overview. *Science* **2002**, *295*, 1662−1664.
(16) Davis, S. A.; Dujardin, E.; Mann, S. Biomolecular Inorganic Materials Chemistry. *Curr. Opin. Solid State Mater. Sci.* **2003**, *7*, 273−281.
(17) Hood, L.; Heath, J. R.; Phelps, M. E.; Lin, B. Systems Biology and New Technologies Enable Predictive and Preventative Medicine. *Science* **2004**, *306*, 640−643.
(18) Ziegler, C. Cantilever-Based Biosensors. *Anal. Bioanal. Chem.* **2004**, *379*, 946−959.
(19) Patwardhan, S. V.; Patwardhan, G.; Perry, C. C. Interactions of Biomolecules with Inorganic Materials: Principles, Applications and Future Prospects. *J. Mater. Chem.* **2007**, *17*, 2875−2884.
(20) Monti, S.; Prampolini, G.; Barone, V. Interactions of Nucleotide Bases with Decorated Si Surfaces from Molecular Dynamics Simulations. *J. Phys. Chem. C* **2011**, *115*, 9146−9156.
(21) Fornaro, T.; Brucato, J. R.; Branciamore, S.; Pucci, A. Adsorption of Nucleic Acid Bases on Magnesium Oxide (MgO). *Int. J. Astrob.* **2013**, *12*, 78−86.
(22) Fornaro, T.; Brucato, J. R.; Pace, E.; Guidi, M. C.; Branciamore, S.; Pucci, A. Infrared Spectral Investigations of {UV} Irradiated Nucleobases Adsorbed on Mineral Surfaces. *Icarus* **2013**, *226*, 1068−1085.
(23) Walcarius, A.; Minteer, S. D.; Wang, J.; Lin, Y.; Merkoci, A. Nanomaterials for Bio-functionalized Electrodes: Recent Trends. *J. Mater. Chem. B* **2013**, *1*, 4878−4908.
(24) Saenger, W., Jeffrey, G. *Hydrogen Bonding in Biological Structures*; Springer-Verlag: Berlin Heidelberg, Germany, 1991.
(25) Robertson, E. G.; Simons, J. P. Getting Into Shape: Conformational and Supramolecular Landscapes in Small Biomolecules and their Hydrated Clusters. *Phys. Chem. Chem. Phys.* **2001**, *3*, 1−18.
(26) de Vries, M. S.; Hobza, P. Gas-phase Spectroscopy of Biomolecular Building Blocks. *Annu. Rev. Phys. Chem.* **2007**, *58*, 585−612.

DOI: 10.1021/acs.jpca.5b01561
J. Phys. Chem. A 2015, 119, 4224−4236

(27) Garand, E.; Kamrath, M. Z.; Jordan, P. A.; Wolk, A. B.; Leavitt, C. M.; McCoy, A. B.; Miller, S. J.; Johnson, M. A. Determination of Noncovalent Docking by Infrared Spectroscopy of Cold Gas-Phase Complexes. *Science* **2012**, *335*, 694−698.
(28) Fornaro, T., Carnimeo, I. *Reference Module in Chemistry, Molecular Sciences and Chemical Engineering*; Elsevier: Amsterdam, 2014; DOI: 10.1016/B978-0-12-409547-2.11025-X.
(29) Sivakova, S.; Rowan, S. J. Nucleobases as Supramolecular Motifs. *Chem. Soc. Rev.* **2005**, *34*, 9−21.
(30) Sowerby, S. J.; Heckl, W. M. The Role of Self-Assembled Monolayers of the Purine and Pyrimidine Bases in the Emergence of Life. *Origins Life Evol. B* **1998**, *28*, 283−310.
(31) Drummond, T. G.; Hill, M. G.; Barton, J. K. Electrochemical DNA Sensors. *Nat. Biotechnol.* **2003**, *21*, 1192−1199.
(32) Levicky, R.; Horgan, A. Physicochemical Perspectives on DNA Microarray and Biosensor Technologies. *Trends Biotechnol.* **2005**, *23*, 143−149.
(33) Singh, P.; Kumar, J.; Toma, F. M.; Raya, J.; Prato, M.; Fabre, B.; Verma, S.; Bianco, A. Synthesis and Characterization of Nucleobase-Carbon Nanotube Hybrids. *J. Am. Chem. Soc.* **2009**, *131*, 13555−13562.
(34) Lee, J.-H.; Choi, Y.-K.; Kim, H.-J.; Scheicher, R. H.; Cho, J.-H. Physisorption of DNA Nucleobases on h-BN and Graphene: vdW-Corrected DFT Calculations. *J. Phys. Chem. C* **2013**, *117*, 13435−13441.
(35) Howorka, S. DNA Nanoarchitectonics: Assembled DNA at Interfaces. *Langmuir* **2013**, *29*, 7344−7353.
(36) Nir, E.; Plützer, C.; Kleinermanns, K.; de Vries, M. Properties of Isolated DNA Bases, Base Pairs and Nucleosides Examined by Laser Spectroscopy. *Eur. Phys. J. D* **2002**, *20*, 317−329.
(37) Plutzer, C.; Hunig, I.; Kleinermanns, K. Pairing of the Nucleobase Adenine Studied by IR-UV Double-resonance Spectroscopy and ab initio Calculations. *Phys. Chem. Chem. Phys.* **2003**, *5*, 1158−1163.
(38) Graindourze, M.; Grootaers, T.; Smets, J.; Zeegers-Huyskens, T.; Maes, G. FT-IR Spectroscopic Study of Uracil Derivatives and Their Hydrogen Bonded Complexes with Proton Donors: Part III. Hydrogen Bonding of Uracils with H_2O in Argon Matrices. *J. Mol. Spectrosc.* **1991**, *243*, 37−60.
(39) Bencivenni, L.; Ramondo, F.; Pieretti, A.; Sanna, N. On the Hydrogen Bonding in Uracil: Its Effect on the Vibrational Spectrum. *J. Chem. Soc., Perkin Trans.* **2000**, *2*, 1685−1693.
(40) Casaes, R. N.; Paul, J. B.; McLaughlin, R. P.; Saykally, R. J.; van Mourik, T. Infrared Cavity Ringdown Spectroscopy of Jet-Cooled Nucleotide Base Clusters and Water Complexes. *J. Phys. Chem. A* **2004**, *108*, 10989−10996.
(41) Choi, M. Y.; Miller, R. E. Multiple Isomers of Uracil-Water Complexes: Infrared Spectroscopy in Helium Nanodroplets. *Phys. Chem. Chem. Phys.* **2005**, *7*, 3565−3573.
(42) Thicoipe, S.; Carbonniere, P.; Pouchan, C. Structural Investigation of Microhydrated Thymine Clusters and Vibrational Study of Isolated and Aqueous Forms of Thymine Using DFT Level of Theory. *Phys. Chem. Chem. Phys.* **2013**, *15*, 11646−11652.
(43) Fornaro, T.; Biczysko, M.; Monti, S.; Barone, V. Dispersion Corrected DFT Approaches for Anharmonic Vibrational Frequency Calculations: Nucleobases and their Dimers. *Phys. Chem. Chem. Phys.* **2014**, *16*, 10112−10128.
(44) Nielsen, H. H. The Vibration-Rotation Energies of Molecules. *Rev. Mod. Phys.* **1951**, *23*, 90−136.
(45) Mills, I. M. In *Molecular Spectroscopy: Modern Research*; Rao, K. N., Mathews, C. W., Eds.; Academic Press: New York, 1972; Chapter Vibration-Rotation Structure in Asymmetric- and Symmetric-Top Molecules, pp115−140.
(46) Carter, S.; Sharma, A. R.; Bowman, J. M.; Rosmus, P.; Tarroni, R. Calculations of Rovibrational Energies and Dipole Transition Intensities for Polyatomic Molecules Using MULTIMODE. *J. Chem. Phys.* **2009**, *131*, 224106.
(47) Christiansen, O. Selected New Developments in Vibrational Structure Theory: Potential Construction and Vibrational Wave Function Calculations. *Phys. Chem. Chem. Phys.* **2012**, *14*, 6672−6687.
(48) Roy, T. K.; Gerber, R. B. Vibrational Self-Consistent Field Calculations for Spectroscopy of Biological Molecules: New Algorithmic Developments and Applications. *Phys. Chem. Chem. Phys.* **2013**, *15*, 9468−9492.
(49) Hermes, M. R.; Hirata, S. Diagrammatic Theories of Anharmonic Molecular Vibrations. *Int. Rev. Phys. Chem.* **2015**, *34*, 71−97.
(50) Bloino, J.; Biczysko, M.; Barone, V. General Perturbative Approach for Spectroscopy, Thermodynamics, and Kinetics: Methodological Background and Benchmark Studies. *J. Chem. Theory Comput.* **2012**, *8*, 1015−1036.
(51) Bloino, J.; Barone, V. A Second-order Perturbation Theory Route to Vibrational Averages and Transition Properties of Molecules: General Formulation and Application to Infrared and Vibrational Circular Dichroism Spectroscopies. *J. Chem. Phys.* **2012**, *136*, 124108.
(52) Barone, V.; Biczysko, M.; Bloino, J.; Borkowska-Panek, M.; Carnimeo, I.; Panek, P. Toward Anharmonic Computations of Vibrational Spectra for Large Molecular Systems. *Int. J. Quantum Chem.* **2012**, *112*, 2185−2200.
(53) Barone, V.; Biczysko, M.; Bloino, J.; Puzzarini, C. Glycine Conformers: A Never-Ending Story? *Phys. Chem. Chem. Phys.* **2013**, *15*, 1358−1363.
(54) Barone, V.; Biczysko, M.; Bloino, J.; Puzzarini, C. Characterization of the Elusive Conformers of Glycine from State-of-the-Art Structural,Thermodynamic, and Spectroscopic Computations: Theory Complements Experiment. *J. Chem. Theory Comput.* **2013**, *9*, 1533−1547.
(55) Olbert-Majkut, A.; Lundell, J.; Wierzejewska, M. Light-Induced Opening and Closing of the Intramolecular Hydrogen Bond in Glyoxylic Acid. *J. Phys. Chem. A* **2014**, *118*, 350−357.
(56) Latouche, C.; Barone, V. Computational Chemistry Meets Experiments for Explaining the Behavior of Bibenzyl: A Thermochemical and Spectroscopic (Infrared, Raman, and NMR) Investigation. *J. Chem. Theory Comput.* **2014**, *10*, 5586−5592.
(57) Reva, I.; Nunes, C. M.; Biczysko, M.; Fausto, R. Conformational Switching in Pyruvic Acid Isolated in Ar and N_2 Matrixes: Spectroscopic Analysis, Anharmonic Simulation, and Tunneling. *J. Phys. Chem. A* **2015**, *119*, 2614−2627.
(58) Dušan, H., Ed. *Theoretical Treatments of Hydrogen Bonding*; John Wiley & Sons: Chichester, U.K., 1997.
(59) del Bene, J. E.; Jordan, M. J. T. Vibrational Spectroscopy of the Hydrogen Bond: an ab initio Quantum-chemical Perspective. *Int. Rev. Phys. Chem.* **1999**, *18*, 119−162.
(60) Buckingham, A. D.; del Bene, J.; McDowell, S. A. C. The Hydrogen Bond. *Chem. Phys. Lett.* **2008**, *463*, 1−10.
(61) Arunan, E.; Desiraju, G. R.; Klein, R. A.; Sadlej, J.; Scheiner, S.; Alkorta, I.; Clary, D. C.; Crabtree, R. H.; Dannenberg, J. J.; Hobza, P.; Kjaergaard, H. G.; Legon, A. C.; Mennucci, B.; Nesbitt, D. J. Defining the hydrogen bond: An account (IUPAC Technical Report). *Pure Appl. Chem.* **2011**, *83*, 1619−1636.
(62) Fornaro, T.; Carnimeo, I.; Biczysko, M. Towards Feasible and Comprehensive Computational Protocol for Simulation of the Spectroscopic Properties of Large Molecular Systems: The Anharmonic Infrared Spectrum of Uracil in the Solid State by Reduced Dimensionality/Hybrid VPT2 Approach. *J. Phys. Chem. A* **2015**, DOI: 10.1021/jp510101y.
(63) Biczysko, M.; Latajka, Z. Accuracy of Theoretical Potential Energy Profiles along Proton-Transfer Coordinate for XH-NH_3 (X=F,Cl,Br) Hydrogen-Bonded Complexes. *J. Phys. Chem. A* **2002**, *106*, 3197−3201.
(64) Becke, A. D. Density-functional Thermochemistry. III. The Role of Exact Exchange. *J. Chem. Phys.* **1993**, *98*, 5648−5652.
(65) Barone, V.; Cimino, P.; Stendardo, E. Development and Validation of the B3LYP/N07D Computational Model for Structural Parameter and Magnetic Tensors of Large Free Radicals. *J. Chem. Theory Comput.* **2008**, *4*, 751−764.

DOI: 10.1021/acs.jpca.5b01561
J. Phys. Chem. A 2015, 119, 4224−4236

(66) Biczysko, M.; Bloino, J.; Carnimeo, I.; Panek, P.; Barone, V. Fully ab initio IR Spectra for Complex Molecular Systems from Perturbative Vibrational Approaches: Glycine as a Test Case. *J. Mol. Struct.* **2012**, *1009*, 74−82.
(67) Carnimeo, I.; Biczysko, M.; Bloino, J.; Barone, V. Reliable Structural, Thermodynamic, and Spectroscopic Properties of Organic Molecules Adsorbed on Silicon Surfaces from Computational Modeling: the Case of Glycine@Si(100). *Phys. Chem. Chem. Phys.* **2011**, *13*, 16713−16727.
(68) Barone, V.; Biczysko, M.; Bloino, J.; Puzzarini, C. Accurate Molecular Structures and Infrared Spectra of trans-2,3-dideuterooxirane, Methyloxirane, and trans-2,3-dimethyloxirane. *J. Chem. Phys.* **2014**, *141*, 034107/1−17.
(69) Carnimeo, I.; Puzzarini, C.; Tasinato, N.; Stoppa, P.; Charmet, A. P.; Biczysko, M.; Cappelli, C.; Barone, V. Anharmonic Theoretical Simulations of Infrared Spectra of Halogenated Organic Compounds. *J. Chem. Phys.* **2013**, *139*, 074310.
(70) Grimme, S.; Antony, J.; Ehrlich, S.; Krieg, H. A Consistent and Accurate ab initio Parametrization of Density Functional Dispersion Correction (DFT-D) for the 94 Elements H-Pu. *J. Chem. Phys.* **2010**, *132*, 154104.
(71) Barone, V.; Biczysko, M.; Pavone, M. The Role of Dispersion Correction to DFT for Modelling Weakly Bound Molecular Complexes in the Ground and Excited Electronic States. *Chem. Phys.* **2008**, *346*, 247−256.
(72) Biczysko, M.; Panek, P.; Barone, V. Toward Spectroscopic Studies of Biologically Relevant Systems: Vibrational Spectrum of Adenine as a Test Case for Performances of Long-range/dispersion Corrected Density Functionals. *Chem. Phys. Lett.* **2009**, *475*, 105−110.
(73) Grimme, S.; Steinmetz, M. Effects of London Dispersion Correction in Density Functional Theory on the Structures of Organic Molecules in the Gas Phase. *Phys. Chem. Chem. Phys.* **2013**, *15*, 16031−16042.
(74) Torres, E.; DiLabio, G. A. A (Nearly) Universally Applicable Method for Modeling Noncovalent Interactions Using B3LYP. *J. Phys. Chem. Lett.* **2012**, *3*, 1738−1744.
(75) DiLabio, G. A.; Koleini, M.; Torres, E. Extension of the B3LYP-dispersion-correcting Potential Approach to the Accurate Treatment of both inter-and Intra-molecular Interactions. *Theor. Chem. Acc.* **2013**, *132*, 1−13.
(76) Carbonniere, P.; Lucca, T.; Pouchan, C.; Rega, N.; Barone, V. Vibrational computations beyond the harmonic approximation: Performances of the B3LYP density functional for semirigid molecules. *J. Comput. Chem.* **2005**, *26*, 384−388.
(77) Begue, D.; Carbonniere, P.; Pouchan, C. Calculations of Vibrational Energy Levels by Using a Hybrid ab Initio and DFT Quartic Force Field: Application to Acetonitrile. *J. Phys. Chem. A* **2005**, *109*, 4611−4616.
(78) Grimme, S. Semiempirical Hybrid Density Functional with Perturbative Second-order Correlation. *J. Chem. Phys.* **2006**, *124*, 034108.
(79) Biczysko, M.; Panek, P.; Scalmani, G.; Bloino, J.; Barone, V. Harmonic and Anharmonic Vibrational Frequency Calculations with the Double-Hybrid B2PLYP Method: Analytic Second Derivatives and Benchmark Studies. *J. Chem. Theory Comput.* **2010**, *6*, 2115−2125.
(80) Papajak, E.; Leverentz, H. R.; Zheng, J.; Truhlar, D. G. Efficient Diffuse Basis Sets: cc-pVxZ+ and maug-cc-pVxZ. *J. Chem. Theory Comput.* **2009**, *5*, 1197−1202.
(81) Truhlar, D. G.; Olson, R. W.; Jeannotte, A. C.; Overend, J. Anharmonic Force Constants of Polyatomic Molecules. Test of the Procedure for Deducing a Force Field from the Vibration-Rotation Spectrum. *J. Am. Chem. Soc.* **1976**, *98*, 2373−2379.
(82) Isaacson, A. D.; Truhlar, D. G.; Scanlon, K.; Overend, J. Tests of Approximation Schemes for Vibrational Energy Levels and Partition Functions for Triatomics: H_2O and SO_2. *J. Chem. Phys.* **1981**, *75*, 3017−3024.
(83) Clabo, D. A., Jr.; Allen, W. D.; Remington, R. B.; Yamaguchi, Y.; Schaefer, H. F., III. A Systematic Study of Molecular Vibrational Anharmonicity and Vibration-Rotation Interaction by Self-Consistent-Fied Higher-Derivative Methods. Asymmetric Top Molecules. *Chem. Phys.* **1988**, *123*, 187−239.
(84) Allen, W. D.; Yamaguchi, Y.; Császár, A. G.; Clabo, D. A., Jr.; Remington, R. B.; Schaefer, H. F., III. A Systematic Study of Molecular Vibrational Anharmonicity and Vibration-Rotation Interaction by Self-Consistent-Fied Higher-Derivative Methods. Linear Polyatomic Molecules. *Chem. Phys.* **1990**, *145*, 427−466.
(85) Amos, R. D.; Handy, N. C.; Green, W. H.; Jayatilaka, D.; Willetts, A.; Palmieri, P. Anharmonic Vibrational Properties of CH_2F_2: A Comparison of Theory and Experiment. *J. Chem. Phys.* **1991**, *95*, 8323−8336.
(86) Maslen, P. E.; Handy, N. C.; Amos, R. D.; Jayatilaka, D. Higher Analytic Derivatives. IV. Anharmonic Effects in the Benzene Spectrum. *J. Chem. Phys.* **1992**, *97*, 4233−4254.
(87) Gaw, F., Willetts, A., Handy, N., Green, W. In *Advances in Molecular Vibrations and Collision Dynamics*; Bowman, J. M., Ed.; JAI Press: Greenwich, CT, 1991; Vol. *1B*, pp 169−185.
(88) Zhang, Q.; Day, P. N.; Truhlar, D. G. The Accuracy of Second Order Perturbation Theory for Multiply Excited Vibrational Energy Levels and Partition Functions for a Symmetric Top Molecular Ion. *J. Chem. Phys.* **1993**, *98*, 4948−4958.
(89) Barone, V. Characterization of the Potential Energy Surface of the HO_2 Molecular System by a Density Functional Approach. *J. Chem. Phys.* **1994**, *101*, 10666−10676.
(90) Barone, V. Anharmonic Vibrational Properties by a Fully Automated Second-order Perturbative Approach. *J. Chem. Phys.* **2005**, *122*, 014108.
(91) Barone, V. Vibrational Zero-Point Energies and Thermodynamic Functions Beyond the Harmonic Approximation. *J. Chem. Phys.* **2004**, *120*, 3059−3065.
(92) Martin, J. M. L.; Lee, T. J.; Taylor, P. M.; François, J.-P. The Anharmonic Force Field of Ethylene, C_2H_4, by Means of Accurate ab initio Calculations. *J. Chem. Phys.* **1995**, *103*, 2589−2602.
(93) Dressler, S.; Thiel, W. Anharmonic Force Fields from Density Functional Theory. *Chem. Phys. Lett.* **1997**, *273*, 71−78.
(94) Stanton, J. F.; Gauss, J. Anharmonicity in the Ring Stretching Modes of Diborane. *J. Chem. Phys.* **1998**, *108*, 9218−9220.
(95) Ruud, K.; Åstrand, P.-O.; Taylor, P.-R. An Efficient Approach for Calculating Vibrational Wave Functions and Zero-point Vibrational Corrections to Molecular Properties of Polyatomic Molecules. *J. Chem. Phys.* **2000**, *112*, 2668−2683.
(96) Ruden, T. A.; Taylor, P. R.; Helgaker, T. Automated Calculation of Fundamental Frequencies: Application to AlH_3 using the Coupled-Cluster Singles-and-Doubles with Perturbative Triples Method. *J. Chem. Phys.* **2003**, *119*, 1951−1960.
(97) Stanton, J. F.; Gauss, J. Analytic Second Derivatives in High-Order Many-Body Perturbation and Coupled-Cluster Theories: Computational Considerations and Applications. *Int. Rev. Phys. Chem.* **2000**, *19*, 61−95.
(98) Neugebauer, J.; Hess, B. A. Fundamental Vibrational Frequencies of Small Polyatomic Molecules from Density-Functional Calculations and Vibrational Perturbation Theory. *J. Chem. Phys.* **2003**, *118*, 7215−7225.
(99) Vázquez, J.; Stanton, J. F. Simple(r) Algebraic Equation for Transition Moments of Fundamental Transitions in Vibrational Second-Order Perturbation Theory. *Mol. Phys.* **2006**, *104*, 377−388.
(100) Vázquez, J.; Stanton, J. F. Treatment of Fermi Resonance Effects on Transition Moments in Vibrational Perturbation Theory. *Mol. Phys.* **2007**, *105*, 101−109.
(101) Barone, V.; Bloino, J.; Guido, C. A.; Lipparini, F. A Fully Automated Implementation of VPT2 Infrared Intensities. *Chem. Phys. Lett.* **2010**, *496*, 157−161.
(102) Krasnoshchekov, S. V.; Isayeva, E. V.; Stepanov, N. F. Numerical-Analytic Implementation of the Higher-Order Canonical Van Vleck Perturbation Theory for the Interpretation of Medium-Sized Molecule Vibrational Spectra. *J. Phys. Chem. A* **2012**, *116*, 3691−3709.

DOI: 10.1021/acs.jpca.5b01561
J. Phys. Chem. A 2015, 119, 4224−4236

(103) Hermes, M. R.; Hirata, S. Second-Order Many-Body Perturbation Expansions of Vibrational Dyson Self-Energies. *J. Chem. Phys.* **2013**, *139*, 034111.
(104) Krasnoshchekov, S. V.; Stepanov, N. F. Nonempirical Anharmonic Vibrational Perturbation Theory Applied to Biomolecules: Free-Base Porphin. *J. Phys. Chem. A* **2015**, *119*, 1616−1627.
(105) Bloino, J. A VPT2 Route to Near-Infrared Spectroscopy: The Role of Mechanical and Electrical Anharmonicity. *J. Phys. Chem. A* **2015**, DOI: 10.1021/jp509985u.
(106) Miani, A.; Cane, E.; Palmieri, P.; Trombetti, A.; Handy, N. C. Experimental and Theoretical Anharmonicity for Benzene Using Density Functional Theory. *J. Chem. Phys.* **2000**, *112*, 248−259.
(107) Burcl, R.; Handy, N. C.; Carter, S. Vibrational Spectra of Furan Pyrrole, and Thiophene from a Density Functional Theory Anharmonic Force Field. *Spectrochim. Acta, Part A* **2003**, *59*, 1881−1893.
(108) Barone, V. Vibrational Spectra of Large Molecules by Density Functional Computations Beyond the Harmonic Approximation: the Case of Pyrrole and Furan. *Chem. Phys. Lett.* **2004**, *383*, 528−532.
(109) Boese, A. D.; Martin, J. Vibrational Spectra of the Azabenzenes Revisited: Anharmonic Force Fields. *J. Phys. Chem. A* **2004**, *108*, 3085−3096.
(110) Barone, V. Accurate Vibrational Spectra of Large Molecules by Density Functional Computations beyond the Harmonic Approximation: The Case of Azabenzenes. *J. Phys. Chem. A* **2004**, *108*, 4146−4150.
(111) Barone, V.; Festa, G.; Grandi, A.; Rega, N.; Sanna, N. Accurate Vibrational Spectra of Large Molecules by Density Functional Computations Beyond the Harmonic Approximation: the Case of Uracil and 2-Thiouracil. *Chem. Phys. Lett.* **2004**, *388*, 279−283.
(112) Charmet, A. P.; Stoppa, P.; Tasinato, N.; Giorgianni, S.; Barone, V.; Biczysko, M.; Bloino, J.; Cappelli, C.; Carnimeo, I.; Puzzarini, C. An Integrated Experimental and Quantum-Chemical Investigation on the Vibrational Spectra of Chlorofluoromethane. *J. Chem. Phys.* **2013**, *139*, 164302.
(113) Grimme, S. Density Functional Theory with London Dispersion Corrections. *Wiley Interdiscip. Rev.: Comput. Mol. Sci.* **2011**, *1*, 211−228.
(114) DiLabio, G. A. Accurate Treatment of Van der Waals Interactions Using Standard Density Functional Theory Methods with Effective Core-Type Potentials: Application to Carbon-containing Dimers. *Chem. Phys. Lett.* **2008**, *455*, 348−353.
(115) Mackie, I. D.; DiLabio, G. A. Interactions in Large, Polyaromatic Hydrocarbon Dimers: Application of Density Functional Theory with Dispersion Corrections. *J. Phys. Chem. A* **2008**, *112*, 10968−10976.
(116) Mackie, I. D.; DiLabio, G. A. Accurate Dispersion Interactions from Standard Density-Functional Theory Methods with Small Basis Sets. *Phys. Chem. Chem. Phys.* **2010**, *12*, 6092−6098.
(117) Zhao, Y.; Truhlar, D. G. The M06 Suite of Density Functionals for Main Group Thermochemistry, Thermochemical Kinetics, Noncovalent Interactions, Excited States, and Transition Elements: Two New Functionals and Systematic Testing of Four M06-class Functionals and 12 Other Functionals. *Theor. Chem. Acc.* **2008**, *120*, 215−241.
(118) Barone, V.; Cimino, P. Accurate and Feasible Computations of Structural and Magnetic Properties of Large Free Radicals: The PBE0/N07D model. *Chem. Phys. Lett.* **2008**, *454*, 139−143.
(119) Barone, V.; Cimino, P. Validation of the B3LYP/N07D and PBE0/N07D Computational Models for the Calculation of Electronic g-Tensors. *J. Chem. Theory Comput.* **2009**, *5*, 192−199.
(120) Double and triple-ζ basis sets of N07 family, are available in the Download section, http://dreams.sns.it (last visited: 1 February, 2015)
(121) Puzzarini, C.; Biczysko, M.; Barone, V. Accurate Anharmonic Vibrational Frequencies for Uracil: The Performance of Composite Schemes and Hybrid CC/DFT Model. *J. Chem. Theory Comput.* **2011**, *7*, 3702−3710.
(122) Biczysko, M.; Bloino, J.; Brancato, G.; Cacelli, I.; Cappelli, C.; Ferretti, A.; Lami, A.; Monti, S.; Pedone, A.; Prampolini, G.; Puzzarini, C.; Santoro, F.; Trani, F.; Villani, G. Integrated Computational Approaches for Spectroscopic Studies of Molecular Systems in the Gas Phase and in Solution: Pyrimidine as a Test Case. *Theor. Chem. Acc.* **2012**, *131*, 1201/1−19.
(123) Puzzarini, C.; Biczysko, M. Microsolvation of 2-Thiouracil: Molecular Structure and Spectroscopic Parameters of the Thiouracil-Water Complex. *J. Phys. Chem. A* **2015**, DOI: 10.1021/jp510511d.
(124) Dapprich, S.; Komáromi, I.; Byun, K.; Morokuma, K.; Frisch, M. J. A new {ONIOM} Implementation in Gaussian98. Part I. The Calculation of Energies, Gradients, Vibrational Frequencies and Electric Field Derivatives. *J. Mol. Struct. Theochem* **1999**, *461−462*, 1−21.
(125) Vreven, T.; Morokuma, K. On the Application of the IMOMO (Integrated Molecular Orbital + Molecular Orbital) Method. *J. Comput. Chem.* **2000**, *21*, 1419−1432.
(126) Boys, S.; Bernardi, F. The Calculation of Small Molecular Interactions by the Differences of Separate Total Energies. Some Procedures with Reduced Errors. *Mol. Phys.* **1970**, *19*, 553−566.
(127) Jurecka, P.; Sponer, J.; Cerny, J.; Hobza, P. Benchmark Database of Accurate (MP2 and CCSD(T) Complete Basis Set Limit) Interaction Energies of Small Model Complexes, DNA Base Pairs, and Amino Acid Pairs. *Phys. Chem. Chem. Phys.* **2006**, *8*, 1985−1993.
(128) Rezac, J.; Riley, K. E.; Hobza, P. S66: A Well-balanced Database of Benchmark Interaction Energies Relevant to Biomolecular Structures. *J. Chem. Theory Comput.* **2011**, *7*, 2427−2438.
(129) Frisch, M. J.; Trucks, G. W.; Schlegel, H. B.; Scuseria, G. E.; Robb, M. A.; Cheeseman, J. R.,; Scalmani, G.; Barone, V.; Mennucci, B.; Petersson, G. A.; et al. *Gaussian 09*, Revision D.01; Gaussian Inc.: Wallingford, CT, 2009.
(130) Licari, D.; Baiardi, A.; Biczysko, M.; Egidi, F.; Latouche, C.; Barone, V. Implementation of a Graphical User Interface for the Virtual Multifrequency Spectrometer: The VMS-Draw Tool. *J. Comput. Chem.* **2015**, *36*, 321−334.
(131) Bouteiller, Y.; Gillet, J.-C.; Grégoire, G.; Schermann, J. P. Transferable Specific Scaling Factors for Interpretation of Infrared Spectra of Biomolecules from Density Functional Theory. *J. Phys. Chem. A* **2008**, *112*, 11656−11660.
(132) Rozenberg, M.; Shoham, G.; Reva, I.; Fausto, R. Low Temperature Fourier Transform Infrared Spectra and Hydrogen Bonding in Polycrystalline Uracil and Thymine. *Spectrochim. Acta, Part A* **2004**, *60*, 2323−2336.
(133) Szczesniak, M.; Nowak, M. J.; Rostkowska, H.; Szczepaniak, K.; Person, W. B.; Shugar, D. Matrix Isolation Studies of Nucleic Acid Constituents. 1. Infrared Spectra of Uracil Monomers. *J. Am. Chem. Soc.* **1983**, *105*, 5969−5976.
(134) Chin, S.; Scott, I.; Szczepaniak, K.; Person, W. B. Matrix Isolation Studies of Nucleic Acid Constituents. 2. Quantitative ab initio Prediction of the Infrared Spectrum of in-plane modes of Uracil. *J. Am. Chem. Soc.* **1984**, *106*, 3415−3422.
(135) Graindourze, M.; Smets, J.; Zeegers-Huyskens, T.; Maes, G. Fourier Transform-Infrared Spectroscopic Study of Uracil Derivatives and Their Hydrogen Bonded Complexes with Proton Donors: Part I. Monomer Infrared Absorptions of Uracil and some Methylated Uracils in Argon Matrices. *J. Mol. Struct.* **1990**, *222*, 345−364.
(136) Puzzarini, C.; Biczysko, M.; Bloino, J.; Barone, V. Accurate Spectroscopic Characterization of Oxirane: A Valuable Route to its Identification in Titan's Atmosphere and the Assignment of Unidentified Infrared Bands. *ApJ.* **2014**, *785*, 107.
(137) Jarmelo, S.; Reva, I.; Carey, P.; Fausto, R. Infrared and Raman Spectroscopic Characterization of the Hydrogen-bonding Network in l-serine Crystal. *Vibr. Spectrosc* **2007**, *43*, 395−404.
(138) Rozenberg, M.; Shoham, G.; Reva, I.; Fausto, R. A Correlation Between the Proton Stretching Vibration Red Shift and the Hydrogen Bond Length in Polycrystalline Amino Acids and Peptides. *Phys. Chem. Chem. Phys.* **2005**, *7*, 2376−2383.

DOI: 10.1021/acs.jpca.5b01561
J. Phys. Chem. A 2015, 119, 4224−4236